A quality survey on different shielding configurations of gamma ray detector used with a portable PGNAA system

E. Bayat [a], H. Afarideh [b,*], F. Abbasi Davani [c], N. Ghal–Eh [d]

[a] Nuclear Science and Technology Research Center, AEOI, Tehran, Iran
[b] Department of Energy Engineering and Physics, Amir Kabir University of Technology, Tehran, Iran
[c] Radiation Application Department, Shahid Beheshti University, Tehran, Iran
[d] School of Physics, Damghan University, Damghan, Iran

HIGHLIGHTS

- A series of shielding sets has been studies for use in a portable PGNAA system.
- An [241]Am–Be source has been used for shielding properties measurement.
- The radiation field components absorbed in shielding material have been measured.
- The best shielding choice has been presented for a portable PGNAA measurement.
- The effect of different HPGe shieldings on the peak areas has been studied.

ARTICLE INFO

ABSTRACT

The appropriate gamma-ray detector shielding configuration is critical for a precise prompt gamma neutron activation analysis (PGNAA) measurement. The shielding material has to prevent the radiation damage to the detector crystal and it must produce less activation gamma rays, whether prompt or delayed, which may interfere the gamma ray spectrum of the sample. In this research, using common shielding materials, a number of combinations have been studies to form a 50 cm long shield for portable PGNAA system against both fast and slow neutrons as well as gamma rays emitted by 20Ci Am–Be source. The measurement results show that in contrast with conventional shadow cone in which the shielding material starts with 20 cm heavy metals such as iron and ends with 30 cm polymer materials, in portable PGNAA systems, the shielding material gives better results if it starts with about 40 cm bo-rated polymer material and ends with an appropriate thickness (7 cm to 10 cm) of heavy metal such as tungsten.

1. Introduction

The use of neutron activation prompt gamma rays for the analysis of materials or PGNAA are extensively used in variety of applications such as luggage inspections to locate explosives, identification of chemical – from non-chemical explosive remnants of war, land-mine detection, real-time cement analysis, etc. (Odena et al., 2006; Charbucinski et al., 2003; Lim and Abernethy, 2005; Gozani and Strellis, 2007; Bergaoui et al., 2014). A PGNAA system basically include neutron source, gamma-ray detector,

spectrum analysis software, electronic modules and appropriate shielding configuration. Here, the shielding is supposed to protect the gamma ray detector from neutrons and as well as the operator from both gamma rays and neutrons. However, in some PGNAA applications such as well-logging tools and the identifications of old explosive remnants, the shielding for operator is normally removed and only the gamma-ray detector is protected (Clifford et al., 2007; Brown and Gozani, 1997). Also in another application where the scattered neutrons off the laboratory walls are studied, one has to shield the detector against direct source neutron irradiation with a so-called shadow cone. The shadow cones are normally made of a combination of heavy elements (such as iron, lead or tungsten to slow down fast neutrons), hydrogenous

---

* Corresponding author. Fax: +98 21 66495519.
  E-mail address: hafarideh@aut.ac.ir (H. Afarideh).

material (such as paraffin or polyethylene) and thermal neutron absorber elements (such as boron or lithium) (Wielopolski et al., 2008). The shielding thickness varies with the neutron source strength and average neutron energy but it is common to use a 50 cm thick shield in most calibration sources (Hara et al., 1987; Johnson, 1979) and also in some PGNAA setups (Hassan et al., 1982).

Several considerations should be taken into account when designing an effective shielding for gamma detector in portable PGNAA systems. For example, the energy resolution of most inorganic scintillators and solid–state semi–conductor detectors are deteriorated due to radiation damage when exposed to a large fluence of fast neutrons ($> 10^8$ n/cm^2 for n-type HPGe detectors) (Raudorf et al., 1984, EG&G ORTEC, 1987). The use of neutron moderator and then a thermal neutron absorber is a frequently-used option for fast neutron shielding, however, in some cases, the thermal neutron absorbers (e.g., gadolinium) produce a large number of secondary gamma rays, which is a real disadvantage when PGNAA on small samples are carried out. The total thickness of shielding material is also an important factor. Although the gamma-ray detectors are more radiation-protected when thicker shielding set is used, the high shielding weight together with low signal-to-noise ratio (as fewer neutrons are received by the sample) are two important draw backs. Therefore, in some cases, to improve the signal-to-noise ratio one has to change the shielding thickness or even change the whole measurement configuration which requires detailed information on the arrangement of different shielding materials (Caffrey et al., 1994).

In this study, to protect an HPGe detector in a portable PGNAA system against a 20Ci ^{241}Am–Be combined neutron–gamma source of 4.4×10^7 n/s neutron yield, a 50-cm long cylindrical shield has been constructed as seen in Fig. 1. This length is generally determined in a trade-off between the radiation damage of HPGe detector(which mainly affects the detection resolution) and its signal-to-noise ratio. The optimum arrangement of the proposed shielding materials may be found by replacing the HPGe with different neutron/gamma-ray detectors to determine the contributions of fast and slow neutrons as well as gamma rays.

2. Materials and methods

The shielding materials used for a 50 cm shield have been iron, tungsten, lead, polyethylene and borated-polyethylene of different boron contents (1, 5 and 30 weight percent). Although a large number of possible permutations of material types and thicknesses exist, as far as our research requirements are concerned, 9 different configurations (as listed in Table 1) have been investigated. All configurations have been set at 95 cm above the room floor and about 2m far from the surrounding walls. The

Table 1
The proposed shielding configurations starting from source side.

Shield number	Materials	Weight (kg)
Set1	Air	0
Set2	1% BPE (20.7 cm)–5% BPE (19.8 cm)–30% BPE (10 cm)	5.7
Set3	Pb (18.8 cm)–1% BPE (20.7 cm)–5% BPE (7.5 cm)–30% BPE (2.5 cm)	26.3
Set4	Pb (50 cm)	60.7
Set5	Pb (12.7 cm)–1% BPE (15.7 cm)–5% BPE (9.8 cm)–30% BPE (5 cm)–Pb (6.9 cm)	27.4
Set6	1% BPE (20.7 cm)–5% BPE (12.2 cm)–30% BPE (7.5 cm)–Pb(9.5 cm)	16.3
Set7	Fe (18.5 cm)–PE (31.5 cm)	22.4
Set8	PE (31.5 cm) – Fe (18.5 cm)	22.4
Set9	1% BPE (20.7 cm)–5% BPE (17.5 cm)–30% BPE (5 cm) – W (6.3 cm)	16.3
Set10	W (6.3 cm)–1% BPE (20.7 cm)–5% BPE (17.5 cm)–30% BPE (5 cm)	16.3

1% BPE and PE stand for 1% borated polyethylene and pure polyethylene, respectively.
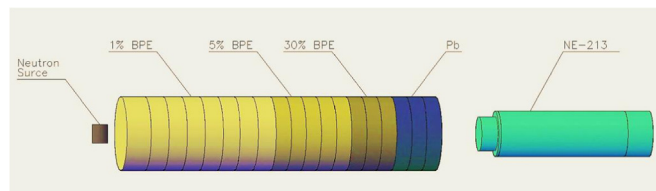

Fig. 2. A schematic of shielding configuration (Set 6).

neutron source-to-detector distance (63 cm) remained unchanged to ensure that the contribution of neutron scatterings at the room floor and nearby walls remains constant. Since all measurements are relative, the detection efficiencies are not included. A schematic of geometry setting is shown in Fig. 2.

In order to study the fast neutron absorption of the proposed shielding configurations, a Ø2″ × 2″ NE213 scintillator together with neutron–gamma discrimination circuitry have been prepared which utilizes zero-crossing method as shown in Fig. 3 (Bayat et al., 2012). The energy calibration has been made by Compton edge of ^{22}Na spectrum (Knox and Miller, 1972). In order to suppress the electronic noise and improve the neutron–gamma discrimination factor (Figure of Merit or FoM), a 300 keVee (i.e., kilo–electronvolt, electron equivalent energy) bias has been set. The live time has been set as 3600s. The neutron energy spectrum has been then obtained with unfolding software, FORIST code (Johnson et al., 1977). The response functions and the detector response matrix have been constructed using O5S (Textor and Verbinski, 1968) and RESPMG (Burrus and Freestone, 1969) codes for which an approximate neutron energy bias of 1.5 MeV has been considered. A 2-in diameter, spherical BF3 detector, LND2708, with 1 cps/nV sensitivity has been responsible for thermal neutron counting in 1000s live time (Fig. 2). The measurement on the gamma rays passing through the proposed shield has been undertaken with a Ø3″ × 3″ BGO scintillator within a live time of 600 s. The background gamma–rays have been suppressed using a 2.5 cm thick bismuth cylinder around the detector.

A one-liter sample of chlorine compound (chloroform from Merck) due to its wide energy range of prompt and delay gamma rays from 517 keV to 7414 keV has been considered for comparing activation measurements in different shield configurations. An n-type HPGe detector of 40% relative efficiency together with a standard spectroscopy modules have been used for measuring prompt gamma rays of neutron-irradiated sample for 300 s live
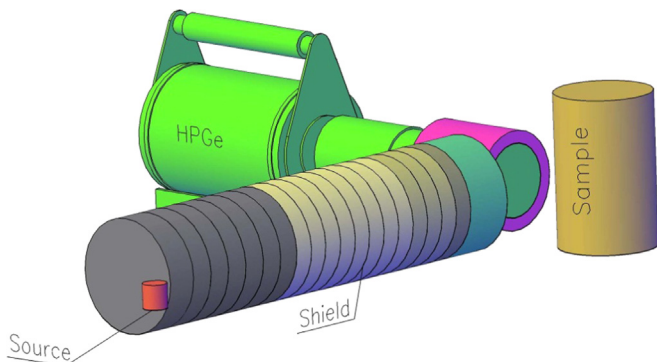

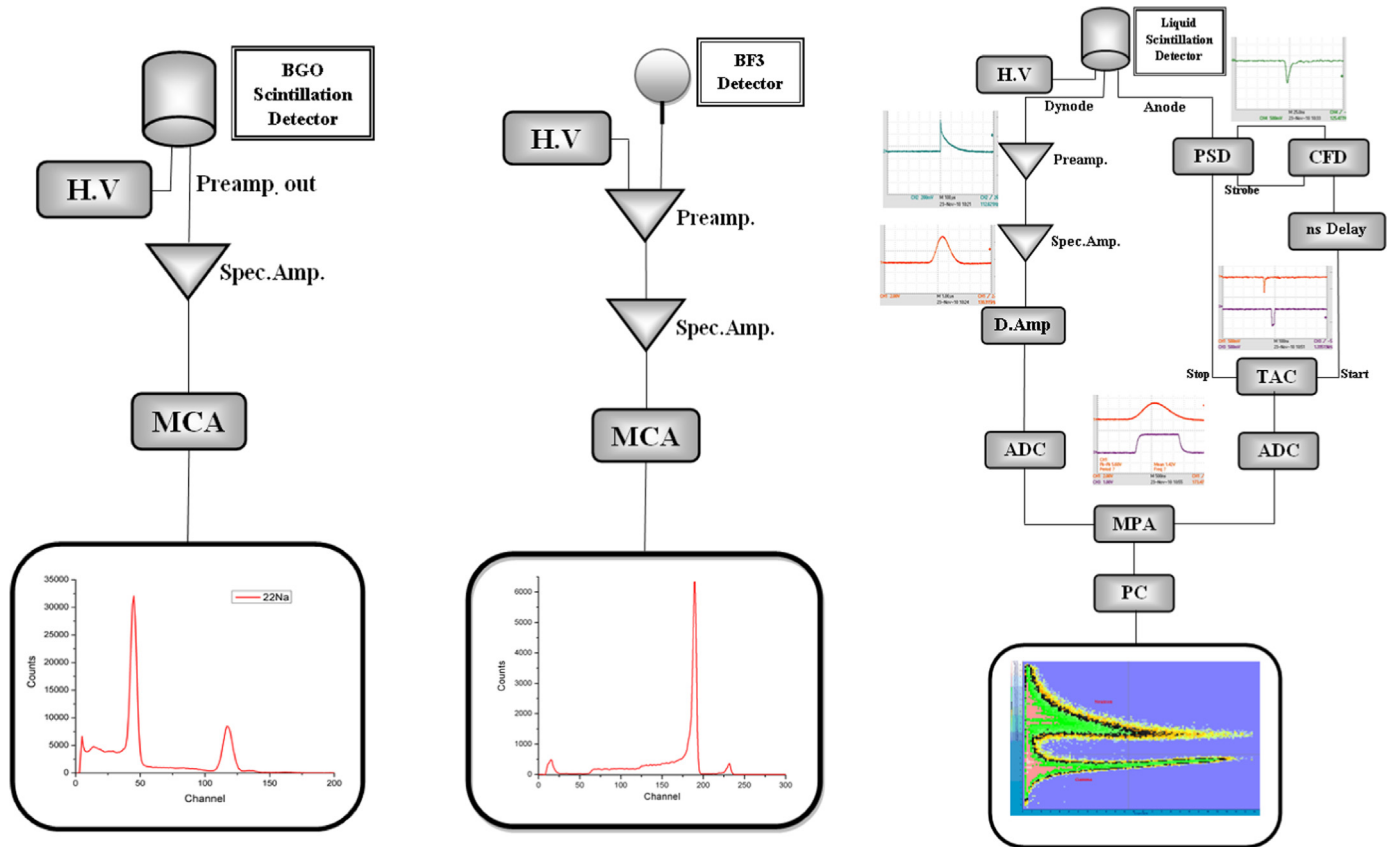**Fig. 1.** A schematic of portable PGNAA system.

Fig. 3. BGO scintillator measurement setup (Left), BF$_3$ counter components (Middle), Neutron–gamma discrimination circuitry used with an NE213 scintillator (Right).
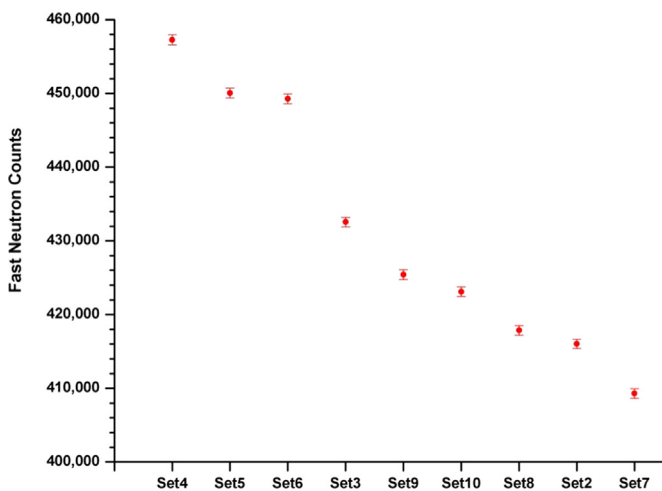

Fig. 4. The NE-213 detector counts associated with fast neutrons passing through different shielding configurations when exposed to an Am–Be source of 20Ci activity (Errors are less than 0.7%).
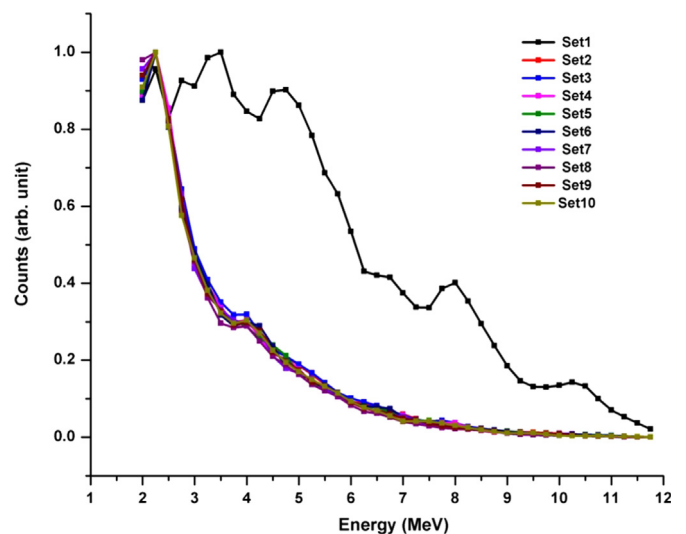

Fig. 5. The spectra of Am–Be neutrons when passed through different shielding configurations (Normalized to maximum-value of each spectrum).

time to obtain the area under chlorine gamma ray peaks.

3. Results and discussion

As shown in Fig. 4, the large neutron interaction cross-section of iron together with good moderation quality of polyethylene causes the shielding Set 7 to exhibit the best performance against fast neutrons. The important point is that the proposed configurations sets have a maximum difference of 10% for fast neutrons shielding. The unfolded spectra of Fig. 5 show that the proposed

shielding configurations have similar smoothing effect on the neutron spectrum and also they move the high-energy neutrons to lower energy regions in similar manner. As seen in Fig. 6, the shielding sets corresponding to those with borated polyethylene, as anticipated, exhibit higher slow neutron absorption properties.

A seen in Fig. 7, the measurement with Set 2 proves that 4.43 MeV gamma rays of Am–Be source has a considerable contribution to total prompt gamma spectrum through Compton scatterings and summation effects (the net summation effect is a rightward displacement of germanium 10.2 MeV capture gamma ray peak). The 478 keV gamma rays originated via $^{10}B(n,\alpha\gamma)^7Li^*$
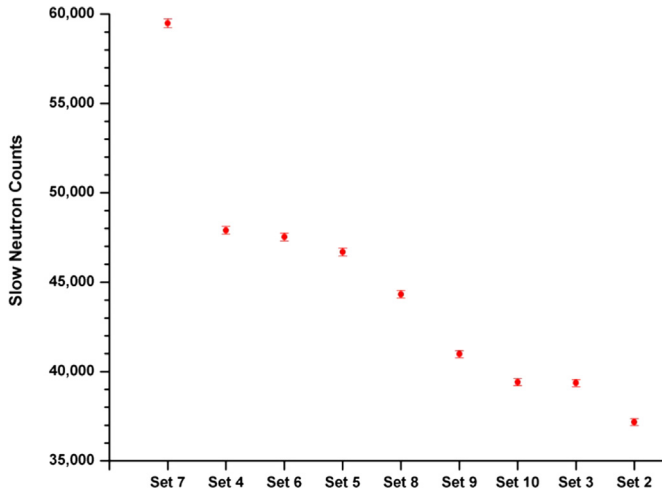
Fig. 6. Slow neutron contribution of Am–Be neutrons when passed through different shielding sets measured with a BF$_3$ counter (Errors are less than 0.28%).

reaction inside borated polyethylene (for shielding sets without heavy element contents at detector side) together with 511 keV annihilation gamma rays form a single peak. Similar spectral behavior can be seen in the prompt gamma spectra of chlorine, as illustrated in Fig. 8, measured with HPGe detector with different shielding sets.

Overall, as shown in Fig. 9, the total transmitted original and secondary gamma rays have their maximum and minimum in polymer shield (Set 2) and those sets with specific lead contents (i.e., Sets 4 and 5), respectively. The area under the 1164 keV prompt gamma ray peak of Fig. 10 may be regarded as a measure to evaluate how effective the proposed shielding are in quantitative analysis.

4. Concluding remarks

The fast neutron component is of prime importance in any shielding configuration when protecting a gamma ray detector against radiation damage (Kubota et al., 1999).The materials and configurations proposed in this study exhibit a maximum difference of 10% for fast neutron counts which means that there is not a significant difference among shielding sets as far as fast neutron shielding is concerned. Therefore, other shielding factors have to be considered for selecting the best shielding set. The thermal neutron interactions with detector materials cause a large number
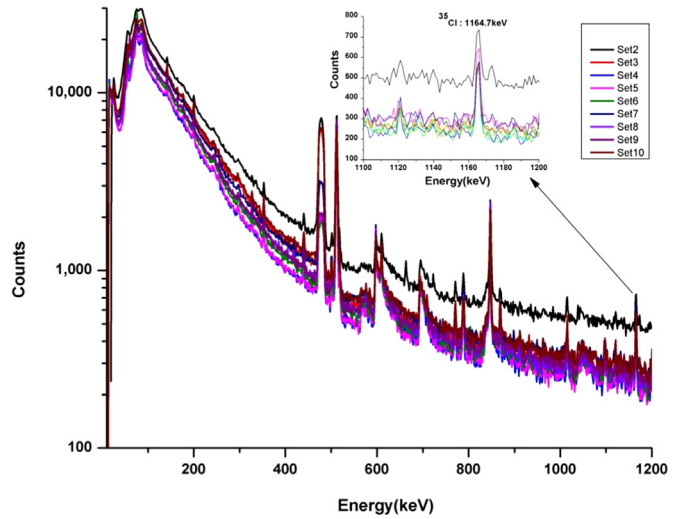

Fig. 8. The prompt gamma spectra of the chlorine sample in 10 keV to 1200 keV energy range recorded with an HPGe detector for different shielding sets.
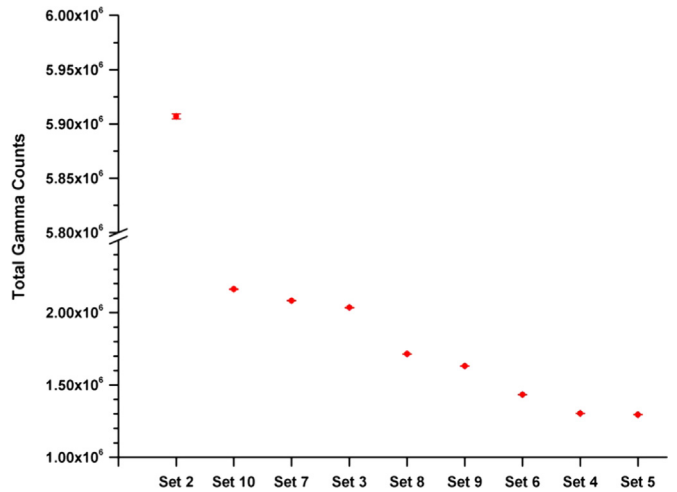

Fig. 9. The total area under the BGO scintillator spectrum for different shielding sets (Errors are less than 0.2%).

of prompt and delay gamma rays which basically increases the dead time, interference with the gamma rays originated from the sample, create summation peak (Biegalski et al., 2006) and the production of impurities in detector crystal. Therefore, the thermal
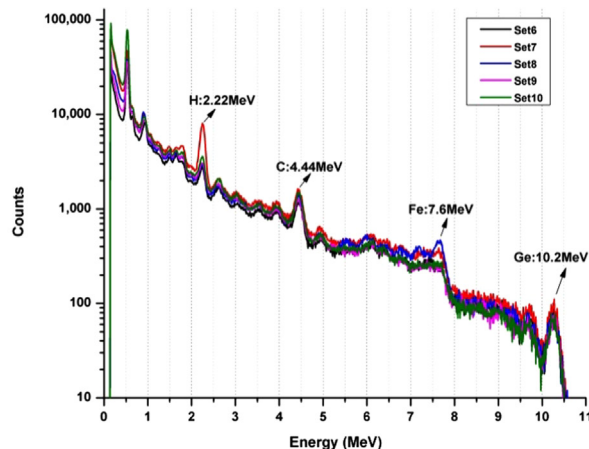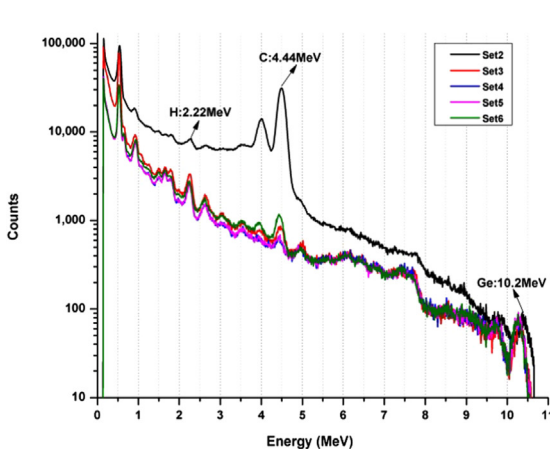

Fig. 7. The single and aggregated gamma rays spectra of both [241]Am–Be and neutron activated shielding material passed through different shielding sets measured with BGO scintillator.
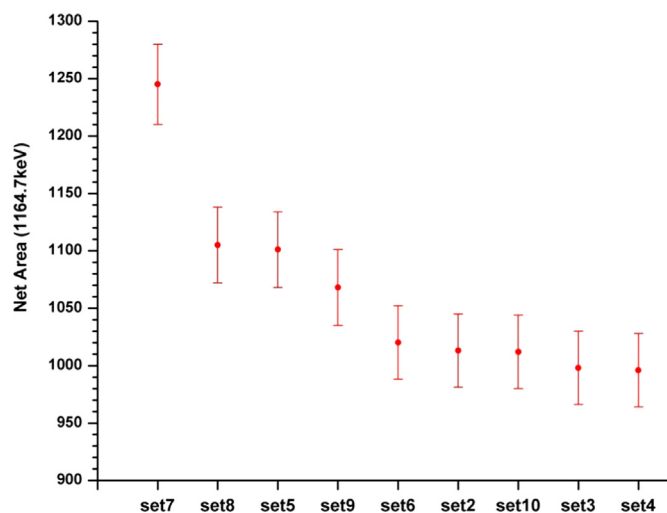
Fig. 10. The area under the chlorine 1164.7 keV gamma-ray peak measured with HPGe detector.

neutrons have to be suppressed as efficiently as possible. The thermal neutrons absorption on the detector is basically checked by comparing the gamma-ray lines produced during the neutron activation of the sample. Here, For example, the area under 198.4 keV gamma ray peak, that is emanated from thermal neutron capture in ^{70}Ge nuclei in HPGe detector (Nikolov et al., 2014), in different shielding sets is in agreement with the total counts of BF_3 counter.

In shielding sets without thermal neutron absorber at the end (e.g., Set 7), the thermal neutron population would increase in detector region that may cause neutron reflections off the sample which increase the number of slow neutrons incident on the detector, as well as the (n,γ) reactions and consequently the gamma-ray counts. One may conclude that to suppress the number of slow neutrons incident on the detector, an appropriate neutron absorber material such as borated polyethylene is required.

The original and secondary gamma rays which are corresponding to source – and neutron-induced gamma rays within shielding material of PGNAA system may interfere with sample gamma rays which reduce the analysis precision (Naqvi et al., 2012). As shown in Fig. 7, the 2223 keV gamma rays produced within polyethylene content of Set 7, reduced the sensitivity of the PGNAA system to the hydrogen nuclei of the sample. Some elements such as iron produce a large number of relatively high-energy gamma rays which disturbs the PGNAA spectrum. The shielding weight is an important factor in a portable setup and has to be chosen as low as possible. It means that the heavy elements such as lead and tungsten which are necessary to decrease both gamma rays and the detector dead time have to be appropriately added. One may conclude that, for a portable PGNAA system, the important parameters are sample type, gamma ray shielding, fast and slow neutron absorption feature and the shielding weight.

Although, it is well understood that the best shielding choice is highly dependent on the application type, the present study proves that Set 9 exhibits the best performance. Although, the shielding used with a PGNAA system has been characterized when using an ^{241}Am–Be source of 4.5 MeV mean energy and relatively high-energy gamma rays of 4.44 MeV, similar shielding behavior is anticipated to be observed for neutron sources with similar neutron yield such as ^{252}Cf and other alpha–Be sources.

References

Bayat, E., Divani–Vais, N., Firoozabadi, M.M., Ghal–Eh, N., 2012. A comparative study on neutron–gamma discrimination with NE213 and UGLLT scintillators using zero-crossing method. Radiat. Phys. Chem. 81, 217–220.

Bergaoui, N., et al., 2014. Monte Carlo simulation of explosive detection system based on a Deuterium–Deuterium (D–D) neutron generator. Appl. Radiat. Isot. 94, 118–124.

Biegalski, S.R., Alvarez, E., Green, T., 2006. Confirmation of germanium interference with hydrogen for prompt gamma–ray activation analysis. Nucl .Instrum. Methods B243, 253–255.

Brown, D.R., Gozani, T., 1997. Thermal neutron analysis technology, cargo inspection system based on pulsed fast neutron analysis. Proc. Int. Soc. Opt. Eng. 2396, 85–94.

Burrus, W.R., Freestone, R.M., 1969. RESPMG: A Response Matrix Generation Code Package, ORNL-TM-2594. Oak Ridge National Lab., Tennessee, U.S.

Caffrey, A.J., et al., 1994. U.S. Army Experience with the PINS Chemical Assay System. EGG–NRP–11443.

Charbucinski, J., Malos, J., Rojc, A., Smith, C., 2003. Prompt gamma neutron activation analysis method and instrumentation for copper grade estimation in large diameter blast holes. Appl. Radiat. Isot. 59, 197–203.

Clifford, E.T.H., McFee, J.E., Ing, H., Andrews, H.R., Tennant, D., Harper, E., Faust, A.A., 2007. A militarily fielded thermal neutron activation sensor for landmine detection. Nucl. Instrum. Methods A579, 418–425.

EG&G ORTEC, 1987. Solid–state Photon Detector Operation Manual of Gamma–X plus Series. EG&G ORTEC GMX–1585–plus, USA.

Gozani, T., Strellis, D., 2007. Advances in neutron based bulk explosive detection. Nucl. Instrum. Methods B261, 311–315.

Hara, A., Iwai, S., Nakamura, T., 1987. Establishment of a simple neutron calibration field from a moderated ^{252}Cf source. Nucl. Instrum. Methods A254, 151–158.

Hassan, A.M., El–Kady, A., El–Ezaby, B., 1982. A prompt gamma-ray system for elemental analysis of complex samples. Nucl. Instrum. Methods A192, 595–601.

Knox, H.H., Miller, T.G., 1972. A technique for determining bias settings for organic scintillators. Nucl. Instrum. Methods A101, 519–525.

Johnson, F.A., 1979. The side-on response of a standard long counter to fast neutrons. Nucl. Instrum. Methods A158, 169–174.

Johnson, R.H., Ingersoll, D.T., Wehring, B.W., Dorning, J.J., 1977. NE213 neutron spectrometry system for measurements from 1.0 to 20 MeV. Nucl. Instrum. Methods A145, 337–346.

Kubota, S., Shiraishi, F., Takami, Y., 1999. Radiation damage of NaI(Tl) by fast neutron irradiation: blocking of the energy transfer processes from V k centers and electrons to the activator of Tl. J. Phys. Soc. Jpn. 68, 298–302.

Lim, C.S., Abernethy, D.A., 2005. On-line coal analysis using fast neutron–induced gamma-rays. Appl. Radiat. Isot. 63, 697–704.

Naqvi, A.A., Al–Matouq, Fares A., Khiari, F.Z., Isab, A.A., Khateeb–urRehman, Raashid, M., 2012. Prompt gamma tests of LaBr$_3$:Ce and BGO detectors for detection of hydrogen, carbon and oxygen in bulk samples. Nucl. Instrum. Methods A684, 82–87.

Nikolov, J., et al., 2014. Applicability of the Ge(n,γ) reaction for estimating thermal neutron flux. Phys. Procedia 59, 71–77.

Odena, C.P., Schweitzerc, J.S., McDowell, G.M., 2006. The feasibility of well-logging measurements of arsenic levels using neutron-activation analysis. Appl. Radiat. Isot. 64, 1074–1081.

Raudorf, T.W., Trammell, R.C., Wagner, S., 1984. Performance of reverse electrode HPGe coaxial detectors after light damage by fast neutrons. IEEE Trans. Nucl. Sci. 31, 253–257 (CONF–831015).

Textor, R.E., Verbinski, V.V., 1968. O5S: A Monte Carlo code for calculating pulse height distributions due to monoenergetic neutrons incident on organic scintillators, ORNL-4160. Oak Ridge National Lab, Tennessee, U.S.

Wielopolski, L., Mitra, S., Doron, O., 2008. Non-carbon-based compact shadow shielding for 14 MeV neutrons. J. Radioanal. Nucl. Chem. 276, 179–182.